Electronic Supporting Information (ESI)

Activating Intersystem Crossing and Aggregation Coupling by CN-Substitution for Efficient Organic Ultralong Room Temperature Phosphorescence

Jie Yuan,[†‡] Yongrong Wang,[†] Ling Li,[†] Shuang Wang,[†] Xingxing Tang,[†] Honglei Wang,[†]

Mingguang Li,[†] Chao Zheng[†], Runfeng Chen[*†]

[†] *Key Laboratory for Organic Electronics and Information Displays & Jiangsu Key Laboratory for Biosensors, Institute of Advanced Materials (IAM), Jiangsu National Synergistic Innovation Center for Advanced Materials (SICAM), Nanjing University of Posts & Telecommunications, 9 Wenyuan Road, Nanjing 210023, China*

[‡] *Engineering Technology Training Center, Nanjing Institute of Industry Technology, 1 Yangshan North Road, Nanjing 210023, China*

**Email: iamrfchen@njupt.edu.cn*

Table of Contents

Synthesis and characterization

Chemicals and solvents purchased from Aldrich or Acros are of analytical grade and were used without further purification. Unless otherwise noted, reactions were carried out under a dry argon atmosphere using standard Schlenk techniques. ^{1}H and ^{13}C-nuclear magnetic resonance (NMR) spectra were recorded on a Bruker Ultra Shield Plus 400 MHz instrument with $CDCl_3$ as the solvent and tetramethylsilane (TMS) as the internal standard. Chemical shifts (δ) are given in *ppm* in Hz. Splitting patterns were designed as follows: s (singlet), d (doublet) and m (multiplet). Liquid chromatograph mass spectrometer (LC/MS) was performed on an Agilent 6230 Accurate-Mass TOF LC/MS using a mixed solvent of 50 vol% water and 50 vol% methanol as the eluent. High resolution mass spectra were collected by a LCT Premier XE (Waters) HRMS spectrometry.

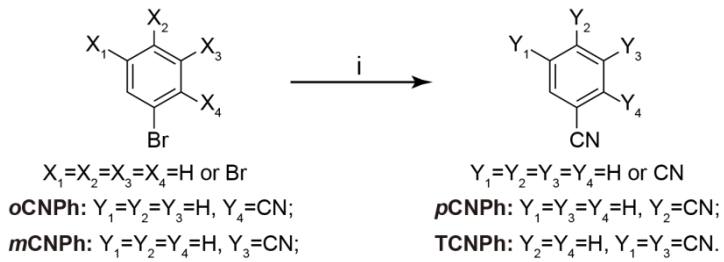

Scheme S1. Synthetic route of the organic afterglow molecules of ***o*CNPh**, ***m*CNPh, *p*CNPh** and **TCNPh**: (i) coppercyanide, N, N-Dimethylformamide, 180ºC, 48 h.

Phthalonitrile (*o*CNPh): To a 250 mL round bottom flask charged with a stir bar was added 1, 2-dibromobenzene (1.17 g, 5.0 mmol), coppercyanide (4.50 g, 50.0 mmol) and 50 mL dry N, N-dimethylformamide. The mixture under argon protection was reacted at 180°C for 48 hours[1]. After cooling to room temperature, the solvent of N, N-dimethylformamide was removed by vacuum distillation. The resulting solid was dissolved in dichloromethane (DCM) and washed with brine. The mixture was then extracted with DCM for three times. The organic phase was collected and dried over $MgSO_4$. After removing the solvent, the crude product was purified by column chromatograph and recrystallized from DCM/hexane for several times to obtain a colorless crystal. Yield: 0.64 g (70%). ^{1}H NMR (400 MHz, $CDCl_3$): δ= 7.88-7.84 (m, 2H), 7.82-7.78 (m, 2H). ^{13}C NMR (100 MHz, $CDCl_3$): δ= 133.62, 133.27, 115.95, 115.40. HRMS ($[M+1]^+$, FAB): calculated

for $C_8H_4N_2$: 129.0374; Found:129.0437.

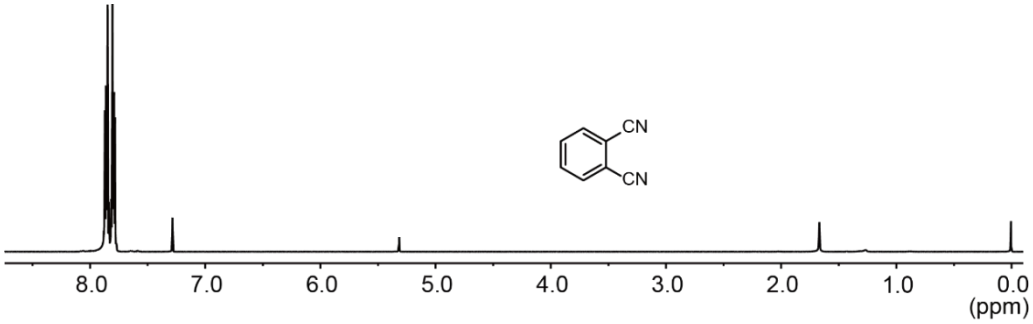

Figure S1. ^{1}H NMR spectrum of phthalonitrile (***o*CNPh**).

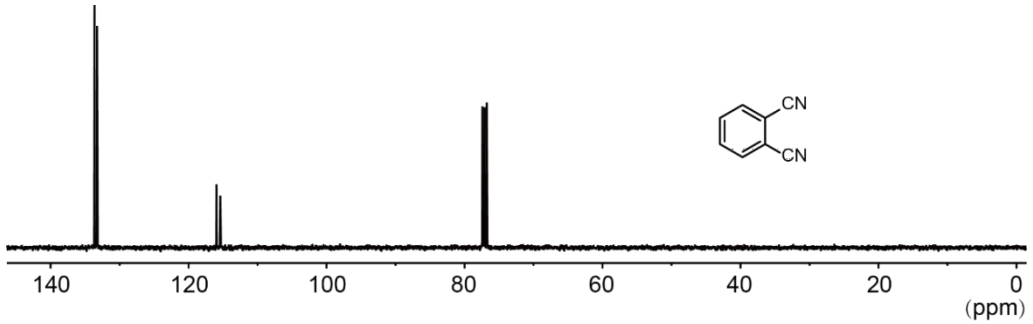

Figure S2. ^{13}C NMR spectrum of phthalonitrile (***o*CNPh**).

Isophthalonitrile (*m*CNPh): Similar to the preparation of ***o*CNPh**, ***m*CNPh** was synthesized by using 1, 3-dibromobenzene (1.17 g , 5.0 mmol). Yield: 0.92 g of colorless crystal (72%). ^{1}H NMR (400 MHz, $CDCl_3$): δ= 7.98-7.91 (m, 3H), 7.70-7.66 (m, 1H). ^{13}C NMR (100 MHz, $CDCl_3$): δ= 136.04, 135.44, 130.38, 116.63, 114.17. HRMS ($[M+1]^+$, FAB): calculated for $C_8H_4N_2$: 129.0374; Found: 129.0440.

Figure S3. ^{1}H NMR spectrum of isophthalonitrile (***m*CNPh**).

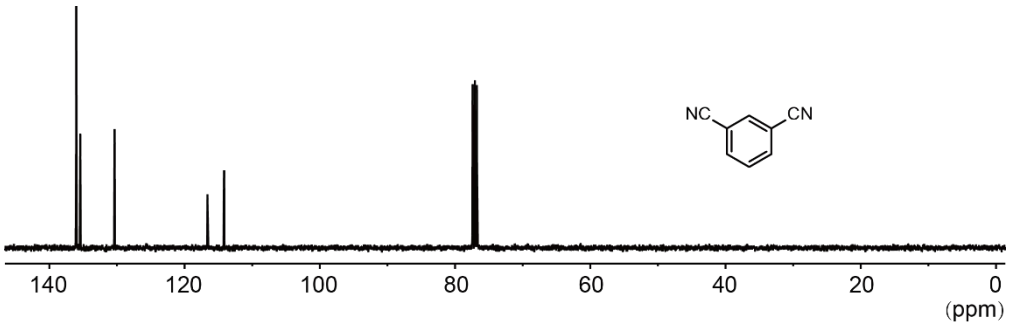

Figure S4. ^{13}C NMR spectrum of isophthalonitrile (***m*CNPh**).

Terephthalonitrile (*p*CNPh): Similar to the preparation of ***o*CNPh**, ***p*CNPh** was synthesized by using 1, 4-dibromobenzene (1.17 g，5.0 mmol). Yield: 0.83 g of colorless crystal (65%). Yield: 0.64 g (70%). ^{1}H NMR (400 MHz, $CDCl_3$): δ= 7.82 (s, 4H). ^{13}C NMR (100 MHz, $CDCl_3$): δ= 132.81, 117.03, 116.74. HRMS ($[M+1]^+$, FAB): calculated for $C_8H_4N_2$: 129.0374; Found: 129.0444.

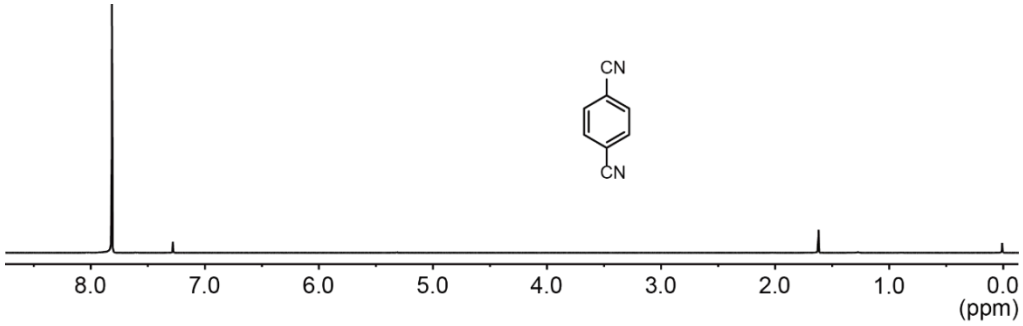

Figure S5. ^{1}H NMR spectrum of terephthalonitrile (***p*CNPh**).

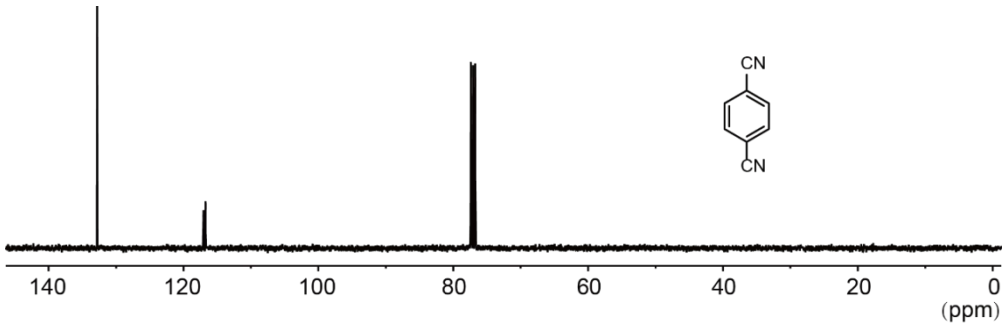

Figure S6. ^{13}C NMR spectrum of terephthalonitrile (***p*CNPh**).

Benzene-1, 3, 5-tricarbonitrile (TCNPh): Similar to the preparation of ***o*CNPh**, **TCNPh** was synthesized by using 1, 3, 5-tribromobenzene (1.56 g，5.0 mmol) and coppercyanide (6.75 g，75.0 mmol). Yield: 0.96 g of colorless crystal (63%). ^{1}H NMR (400 MHz, $CDCl_3$): δ= 8.20 (s, 3H). ^{13}C NMR (100 MHz, $CDCl_3$): δ= 138.67, 115.99, 114.62. HRMS ($[M+1]^+$, FAB): calculated for $C_9H_3N_2$: 153.0327; Found: 153.0446.

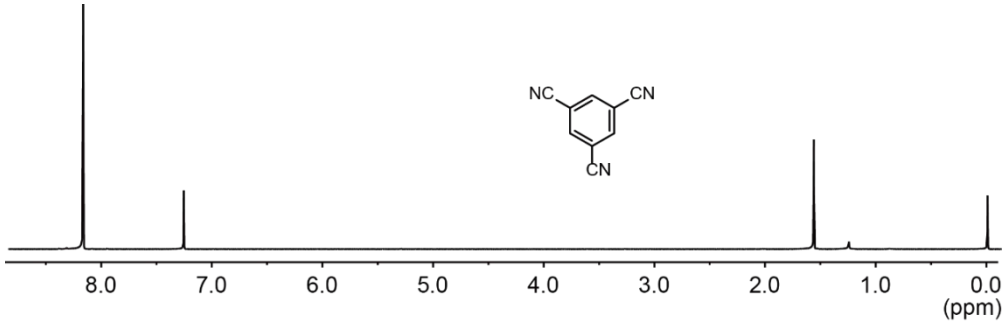

Figure S7. ^{1}H NMR spectrum of benzene-1, 3, 5-tricarbonitrile (**TCNPh**).

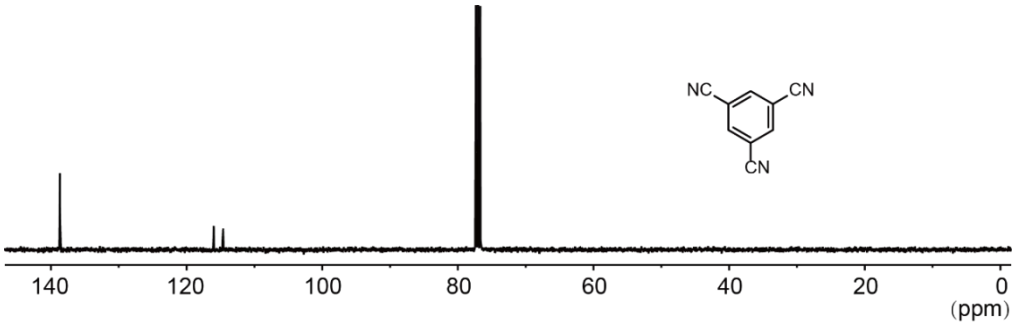

Figure S8. ^{13}C NMR spectrum of benzene-1, 3, 5-tricarbonitrile (**TCNPh**)

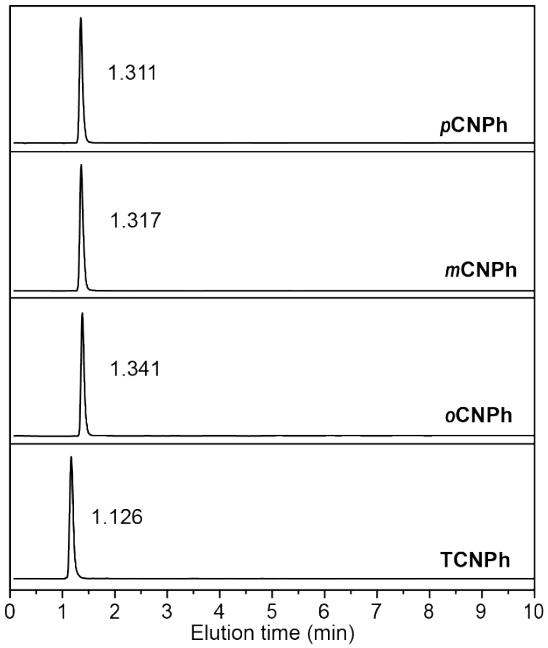

Figure S9. Liquid chromatographs of ***o*CNPh**, ***m*CN Ph, *p*CNPh** and **TCNPh** after the recrystallization.

Single crystal X-ray analysis

Single crystals were grown by slow evaporation of combined DCM and petroleum ether solutions at room temperature. X-ray crystallography was carried out on a Bruker Smart Apex CCD area detector diffractometer using graphite-monochromated Mo-Kα radiation (λ = 0.71073 Å) at 293 K. Cell parameters were retrieved using SMART software and refined using SAINT on all observed reflections. Structures were solved by direct methods using the program SHELX-97 program package. Non-hydrogen atoms were found using alternating difference Fourier syntheses and least-squared refinement cycles and, during the final cycles, were refined anisotropically. Hydrogen atoms were placed in calculated positions and refined as riding atoms with a uniform value of U_{iso}^2. The crystal structure was analyzed by Diamond 3.2 software. Crystallographic parameters of ***o*CNPh**, ***m*CNPh, *p*CNPh** and **TCNPh** were summarized in **Table S1**. CCDC reference numbers for ***o*CNPh**, ***m*CNPh, *p*CNPh** and **TCNPh** are Nos. 1885181, 1885182, 1885183 and 1441873, respectively.

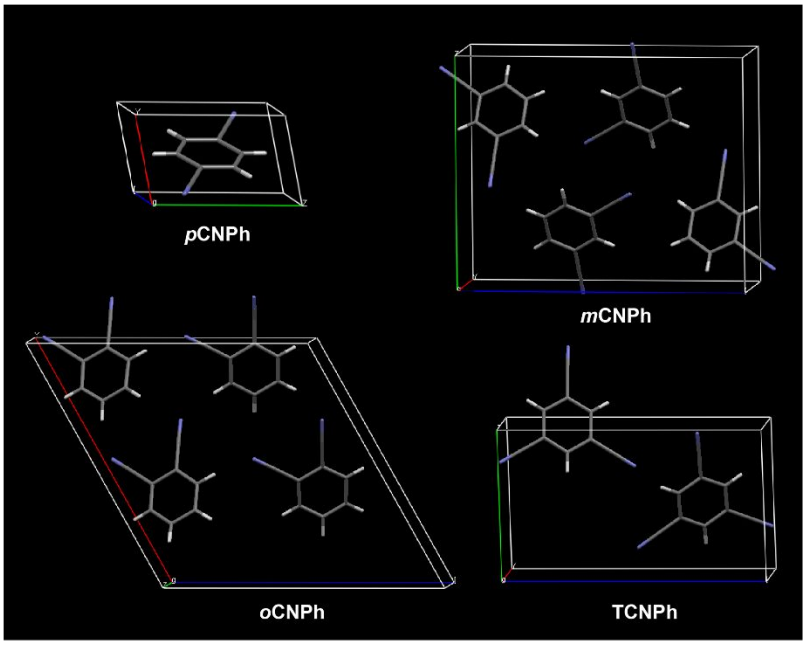

Figure S10. Single-crystal structures of ***o*CNPh**, ***m*CNPh, *p*CNPh** and **TCNPh**.

Table S1. Structure data of benzene (**Ph**), ***p*CNPh**, ***m*CNPh, *o*CNPh** and **TCNPh** single crystals.

Compound	**Ph**[3]	***o*CNPh**	***m*CNPh**	***p*CNPh**	**TCNPh**[4]
Empirical formula	C_6H_6	$C_8H_4N_2$	$C_8H_4N_2$	$C_8H_4N_2$	$C_9H_3N_3$
Formula weight (g mol^{-1})	78.11	128.13	128.13	128.13	153.14
Crystal color	colorless	colorless	colorless	colorless	colorless
Wavelength (Å)	-	0.71073	0.71073	0.71073	0.71073
Space Group	P b c a	Pn	P-1	P-1	P 21
a (Å)	7.390	14.125(14)	3.909(4)	3.781(3)	3.8397(8)
b (Å)	9.42	3.844(4)	11.970(13)	6.450(5)	7.7446(15)
c (Å)	6.81	14.305(15)	14.614(14)	7.270(5)	13.585(3)
α (deg)	90	90	89.88(4)	114.297(13)	90
β (deg)	90	119.046(17)	85.59(3)	92.785(15)	93.79(3)
γ (deg)	90	90	89.86(3)	97.812(16)	90
V (Å^3)	474.07	679.0(12)	681.9(12)	159.02(19)	403.10(14)
Z	4	4	4	1	2
Density (g cm^{-3})	1.094	1.253	1.248	1.338	1.262
μ (mm^{-1})	-	0.079	0.078	0.084	0.081
T_{min}, T_{max}	-	0.991, 0.992	0.945, 0.954	0.904, 0.959	0.972, 0.993
F(000)	69.7	264.0	264.0	66.0	156.0
h_{max}, k_{max}, l_{max}	-	16, 4, 16	5, 13, 18	6, 10, 8	4, 10, 17
$Theta_{max}$	-	24.992	28.071	37.902	27.440

Photophysical property investigations

Ultraviolet-visible (UV-Vis) spectra were measured using a SHIMADZU UV-3600 UV-VIS-NIR spectrophotometer. Steady-state photoluminescence, phosphorescence spectra, and quantum yields were performed on an Edinburgh FLSP920 fluorescence spectrophotometer. For steady-state photoluminescence, time-resolved excitation spectra and quantum yields measurements, a xenon arc lamp (Xe900) was used; Xe900 can provide excellent steady state excitation source. For phosphorescence spectra, a microsecond flash-lamp (uF900) were used; the uF900 flash lamp produces short, typically a few μs, and high irradiance optical pulses for phosphorescence measurements in the range from microseconds to seconds. The LED flash lamp provides subnanosecond optical pulses over the UV-to-vis spectral range for fluorescence decay measurements. The microsecond flash lamp produces short, typically a few microsecond (μs), and high irradiance optical pulses for the organic ultralong room temperature phosphorescence (OURTP) decay measurements. The lifetimes (τ) of the luminescence were obtained by fitting the decay curve with a multi-exponential decay function[5] of

$$I(t) = \sum_i A_i e^{-\frac{t}{\tau}} \tag{S1}$$

where A_i and τ_i represent the amplitudes and lifetimes of the individual components for multi-exponential decay profiles, respectively. The photographs were recorded by a Nikon D90 camera.

One of the most important and experimentally elusive parameters of intramolecular energy transfer is the rate constant for intersystem crossing from the lowest excited singlet to triplet state, k_{ISC}. Experimentally, k_{ISC} can be estimated as follows[6-7]:

$$\frac{\Phi^P}{\tau^F} \le k_{ISC} \le \frac{1-\Phi^F}{\tau^F} \tag{S2}$$

$$k_{ISC}^{min} = \frac{\Phi^P}{\tau^F} \tag{S3}$$

$$k_{ISC}^{max} = \frac{1-\Phi^F}{\tau^F} \tag{S4}$$

where Φ^F and Φ^P represent the photoluminescence quantum yields (PLQY) of fluorescence and phosphorescence, respectively; τ^F represents the lifetime of fluorescence; while k_{ISC}^{min} and k_{ISC}^{max}

are the bottom and upper limits of k_{ISC}, respectively.

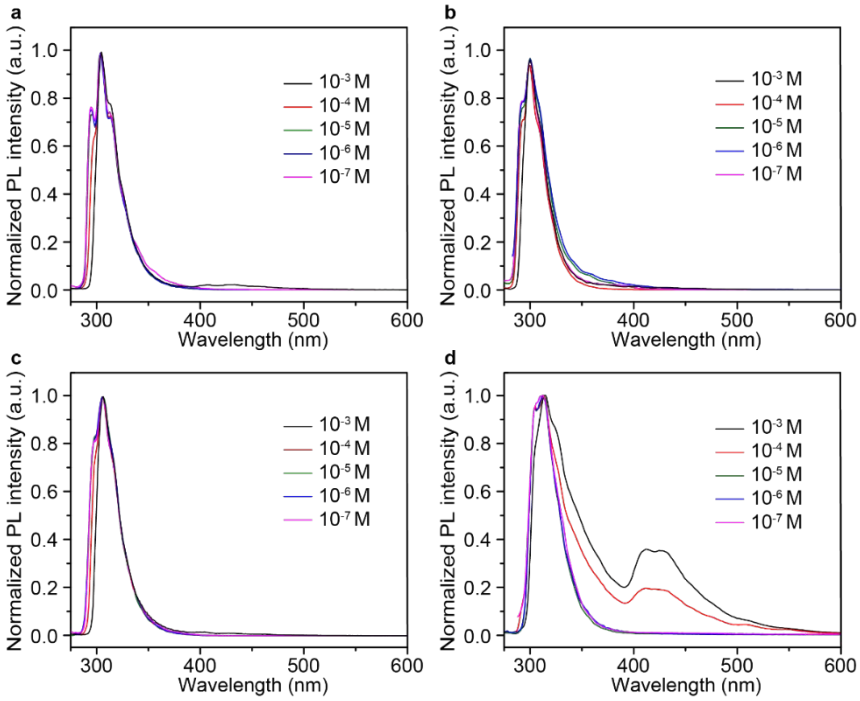

Figure S11. Fluorescence spectra of (a) ***o*CNPh**, (b) ***m*CNPh,** (c) ***p*CNPh** and (d) **TCNPh** in acetonitrile solutions with different concentrations excited by 250 nm at room temperature.

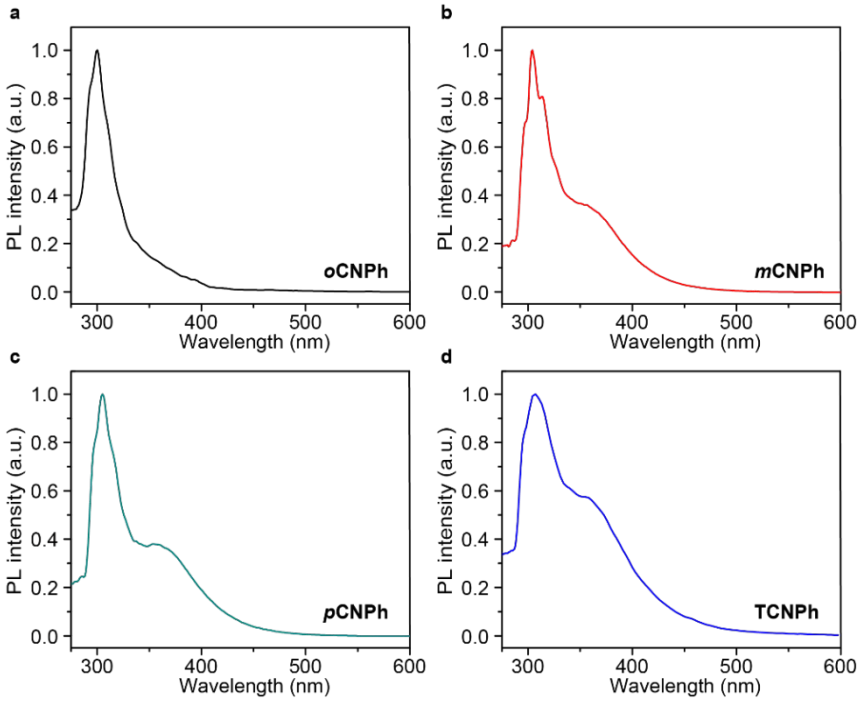

Figure S12. Fluorescence spectra of (a) ***o*CNPh**, (b) ***m*CNPh,** (c) ***p*CNPh** and (d) **TCNPh** (1 wt%) in polymethyl methacrylate (PMMA) under excitation of 250 nm at room temperature.

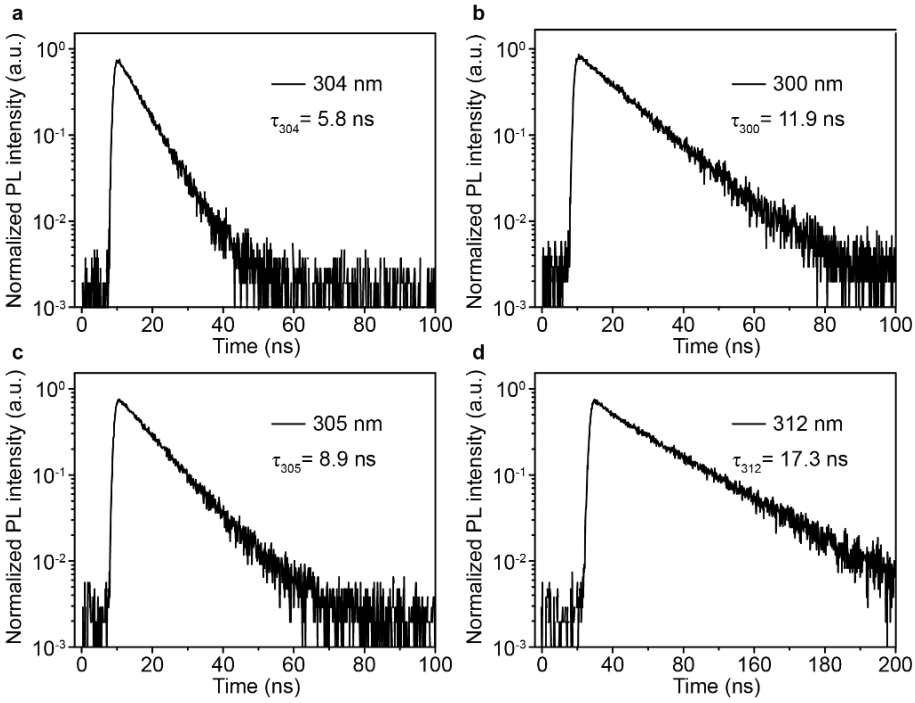

Figure S13. Fluorescence decay curves of ***o*CNPh**, ***m*CNPh, *p*CNPh** and **TCNPh** in dilute acetonitrile solutions (10^{-6} mol L^{-1}) excited by 250 nm irradiation at room temperature.

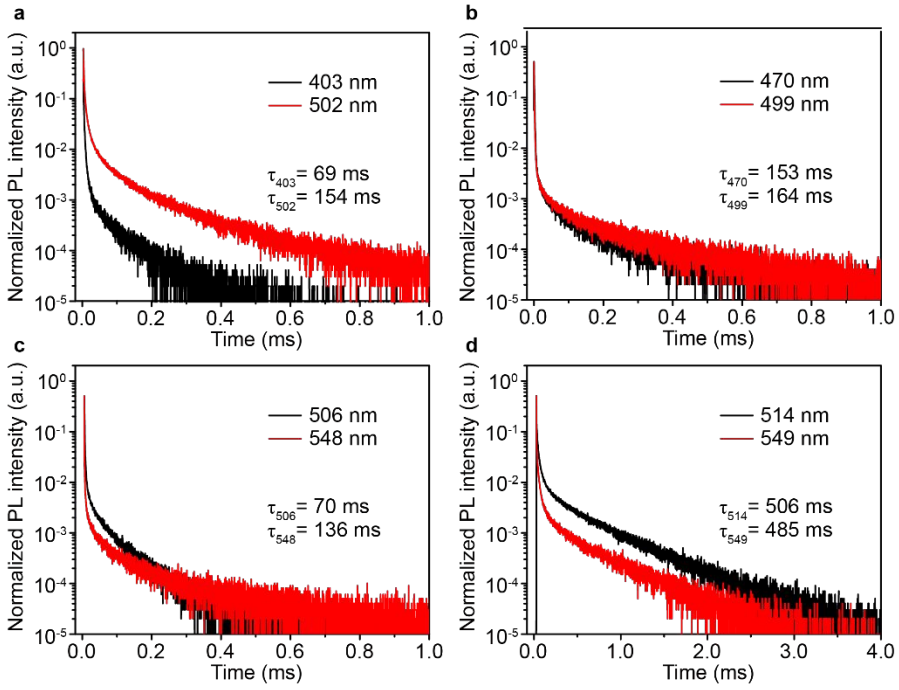

Figure S14. OURTP decay curves of (a) ***o*CNPh**, (b) ***m*CNPh,** (c) ***p*CNPh** and (d) **TCNPh** crystals excited at 290 nm at room temperature.

Table S2. Photoluminescence properties and kinetic parameters of OURTP molecules in dilute acetonitrile solution.

Compound	Fluorescence[a]			Phosphorescence[b]		ISC	
	λ (nm)	τ (ns)	Φ_F (%)	λ (nm)	Φ_P (%)	*k*min ISC (s^{-1})	*k*max ISC (s^{-1})
Ph	286	28	4.1	346	10.5	3.8×10^6	3.4×10^7
***o*CNPh**	304	5.8	19.0	393	48.2	8.3×10^7	1.4×10^8
***m*CNPh**	300	11.9	16.7	372	62.7	5.3×10^7	7.0×10^7
***p*CNPh**	305	8.9	31.2	403	56.0	6.3×10^7	7.7×10^7
TCNPh	312	17.3	15.1	388	47.0	2.7×10^7	4.9×10^7

[a]: at room temperature; [b]: at 77 K.

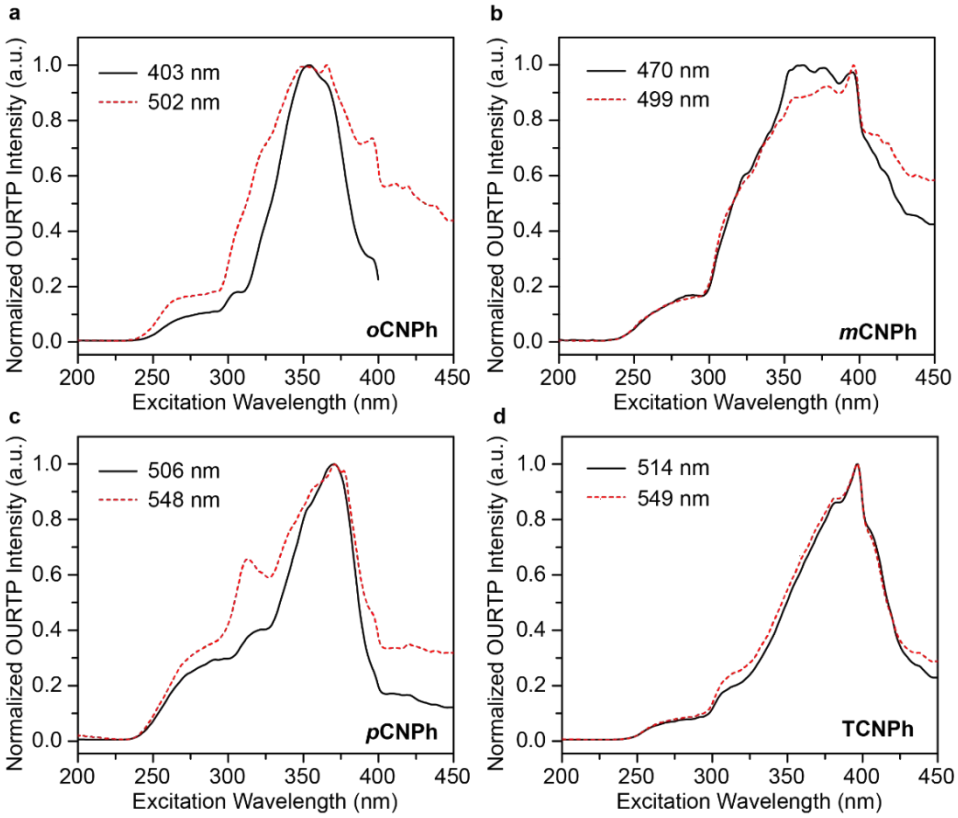

Figure S15. Excitation spectra of OURTP peaks of (a) ***o*CNPh** (403, 502 nm), (b) ***m*CNPh** (470, 499 nm), (c) ***p*CNPh** (506, 548 nm) and (d) **TCNPh** (514, 549 nm) crystals at room-temperature.

Time-dependent density functional theory (TD-DFT) calculations

Density functional theory (DFT) and time-dependent DFT (TD-DFT) calculations were carried out on Gaussian 09 D.01 package[8]. The ground state (S_0) geometry was fully optimized at B3LYP/6-31G(d) level and the optimized stationary point was further characterized by harmonic vibration frequency analysis to ensure that real local minima had been found. The excitation energies in the

n-th singlet (S_n) and triplet (T_n) states were computed using the TD-DFT method based on the optimized molecular structure at the ground state (S_0). Spin-orbit coupling (SOC) matrix elements between the singlet and triplet excited states are calculated with quadratic response function methods using the Dalton program. The SOCs of molecules presented in Table S3 were performed at the optimized geometry at T_1 state using B3LYP functional and 6-31G* basis set[9]. Contour of electrostatic potential (ESP) were obtained also on the ground state geometry to investigate the charge density distribution[10]. The color code of the map was from the deepest red to the deepest blue, when the potential increases in the order of red < orange < yellow < green < blue. The π-π stacked H-aggregated states of the dimers were calculated with B3LYP/6-31G(d) to take into consideration the weak long-range intermolecular interactions. The triplet energy stabilization energy was calculated by the difference between the total molecular energy of the dimer and a sum of the total molecular energy of the two monomers on S_0 and T_1, respectively.

According to the Frenkel exciton theory[11], the $\Delta\varepsilon$ in the case of dimer is given by:

$$\Delta\varepsilon = \frac{2|M|^2}{r_{uv}^3}(\cos\alpha - 3\cos\theta_1\cos\theta_2) \quad \text{(S5)}$$

where M is the electric dipole transition moment, α is the angle between the transition moments of the two molecules in the dimer, and θ_1 and θ_2 are the angles between transition moments of the two molecules and the interconnection of the centers respectively, r_{uv} is the distance between the point dipoles in molecules u and v. As a result, when $\Delta\varepsilon > 0$, it belongs to H-aggregation, and when $\Delta\varepsilon < 0$, it is J-aggregation.

Table S3. TD-DFT-calculated energy levels at singlet (S_1) and triplet (T_n) states and spin-orbit coupling (SOC) results between S_1, S_2 and T_n of **Ph**, ***o*CNPh**, ***m*CNPh, *p*CNPh** and **TCNPh** with $^{\triangle}E_{ST}$ between ±0.37 eV.

Compounds	$S_n \rightarrow T_n$	S_n (eV)	T_n (eV)	ΔE_{ST} (eV)	SOC (cm^{-1})
Ph	$S_1 \rightarrow T_4$	5.54	5.21	0.33	0.01
***o*CNPh**	$S_1 \rightarrow T_4$	4.81	4.69	0.12	0.01
	$S_2 \rightarrow T_5$	4.81	3.17	0.25	5.05
	$S_2 \rightarrow T_6$	5.10	4.70	0.27	2.82
	$S_2 \rightarrow T_7$	5.10	5.44	-0.35	0.17
***m*CNPh**	$S_1 \rightarrow T_4$	4.85	4.62	0.23	0.01
	$S_2 \rightarrow T_5$	5.41	5.40	0.01	0.01
	$S_2 \rightarrow T_6$	5.41	5.61	-0.21	11.40
	$S_2 \rightarrow T_7$	5.41	5.68	-0.28	8.12
	$S_2 \rightarrow T_8$	5.41	3.72	-0.31	0.00
***p*CNPh**	$S_1 \rightarrow T_4$	4.89	4.94	-0.05	14.76
	$S_1 \rightarrow T_5$	4.89	4.98	-0.09	0.02
	$S_2 \rightarrow T_4$	5.10	4.94	0.16	0.58
	$S_2 \rightarrow T_5$	5.10	4.98	0.12	0.02
TCNPh	$S_1 \rightarrow T_4$	4.57	4.38	0.19	0.00
	$S_2 \rightarrow T_5$	5.27	5.08	0.19	0.00
	$S_2 \rightarrow T_6$	5.27	5.08	0.19	0.00
	$S_2 \rightarrow T_7$	5.27	5.56	-0.29	11.39
	$S_2 \rightarrow T_8$	5.27	5.56	-0.29	7.83

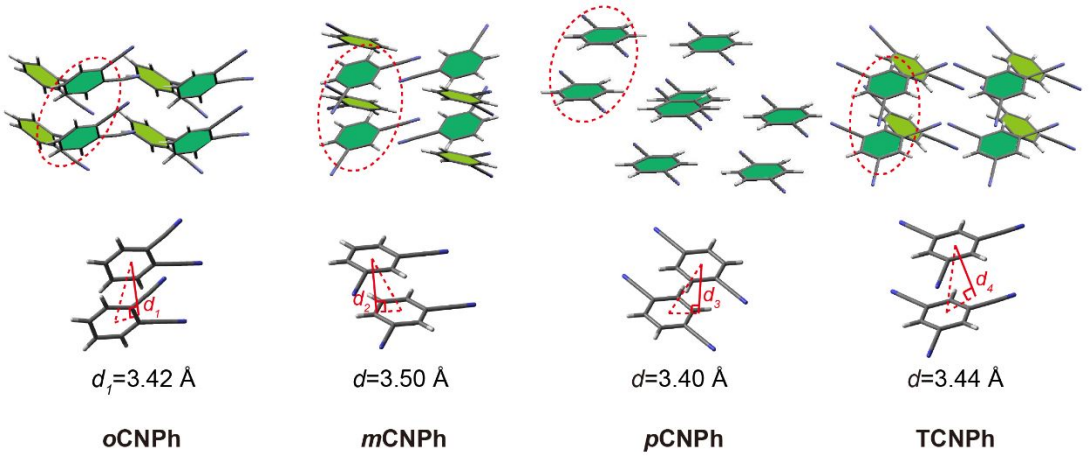

Figure S16. Strong π–π stacking with two phenyl rings paralleling to each other from the single crystals of ***o*CNPh**, ***m*CNPh, *p*CNPh** and **TCNPh**.

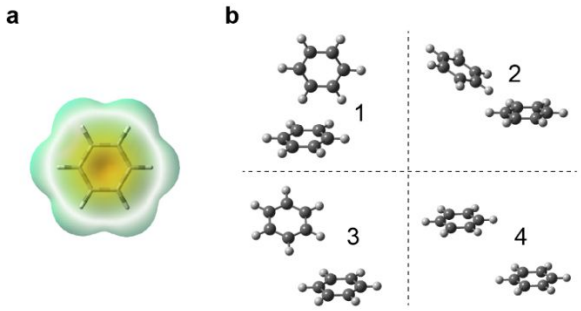

Figure S17. (a) Electrostatic potential (ESP) and (b) molecular pairs involved in the first coordination shell of a given molecule in the crystal structure of benzene at 138 K[12].

Table S4. Aggregation structures in ***o*CNPh**, ***m*CNPh, *p*CNPh** and **TCNPh** dimers in their crystals, and when $\Delta\varepsilon > 0$, it belongs to H-aggregation (in red), and when $\Delta\varepsilon < 0$, it is J-aggregation (in black).

Compounds	Dimer	α (°)	θ_1(°)	θ_2(°)	M (Debye)	r (Å)	$\Delta\varepsilon$ (eV)
***o*CNPh**	5 0	44.6	114.0	108.3	7.27	1.13	1.30×10^{-3}
	5 1	44.6	100.3	117.9	7.76	1.13	1.57×10^{-3}
	5 2	44.6	72.6	66.0	7.27	1.13	1.44×10^{-3}
	5 3	44.6	61.1	78.0	7.76	1.13	1.40×10^{-3}
	5 4	0.0	114.1	114.1	3.84	1.13	1.41×10^{-2}
	5 6	0.0	65.9	65.9	3.84	1.13	1.41×10^{-2}
	5 13	53.1	49.5	73.2	7.72	1.13	1.25×10^{-4}
	5 7	3.0	172.3	172.1	8.03	1.13	-6.02×10^{-3}
	5 8	3.0	154.9	152.0	7.05	1.13	-6.40×10^{-3}
	5 9	3.0	25.0	27.9	7.07	1.13	-6.36×10^{-3}
	5 10	3.0	7.5	7.7	8.05	1.13	-5.97×10^{-3}
	5 11	53.1	61.5	55.5	7.23	1.13	-8.88×10^{-4}
	5 12	53.1	125.8	115.9	7.20	1.13	-7.07×10^{-4}
	5 14	53.1	110.1	130.6	7.70	1.13	-2.43×10^{-4}
***m*CNPh**	5 1	179.7	156.6	23.1	7.20	0.30	4.78×10^{-4}
	5 3	179.7	170.7	9.4	8.21	0.30	4.04×10^{-4}
	5 4	0.0	67.5	67.5	3.91	0.30	1.09×10^{-4}
	5 6	0.0	112.5	112.5	3.91	0.30	1.09×10^{-3}
	5 7	82.0	88.0	157.6	10.17	0.30	2.58×10^{-5}
	5 0	179.7	58.8	121.1	7.56	0.30	-5.31×10^{-5}
	5 2	179.7	68.2	111.9	6.51	0.30	-2.45×10^{-4}
	5 8	82.0	98.3	177.5	7.89	0.30	-6.97×10^{-5}
	5 9	82.0	2.7	81.6	7.89	0.30	-7.08×10^{-5}

	5 10	82.0	111.5	152.3	7.19	0.30	-2.61×10^{-4}
***p*CNPh**	7 0	0.0	99.5	99.5	7.80	0.71	1.21×10^{-3}
	7 2	0.0	66.0	66.0	3.78	0.71	5.79×10^{-3}
	7 4	0.0	112.2	112.2	7.47	0.71	8.52×10^{-4}
	7 6	0.0	62.8	62.8	7.27	0.71	6.03×10^{-4}
	7 8	0.0	117.2	117.2	7.27	0.71	6.03×10^{-4}
	7 10	0.0	67.8	67.8	7.47	0.71	8.52×10^{-4}
	7 12	0.0	114.0	114.0	3.78	0.71	5.79×10^{-3}
	7 14	0.0	80.5	80.5	7.80	0.71	1.21×10^{-3}
	7 1	0.0	52.7	52.7	8.03	0.71	-1.23×10^{-4}
	7 3	0.0	13.3	13.3	7.91	0.71	-2.32×10^{-3}
	7 5	0.0	162.6	162.6	6.45	0.71	-4.02×10^{-3}
	7 9	0.0	17.4	17.4	6.45	0.71	-4.02×10^{-3}
	7 11	0.0	166.7	166.7	7.91	0.71	-2.32×10^{-3}
	7 13	0.0	127.3	127.3	8.03	0.71	-1.23×10^{-4}
TCNPh	11 0	55.7	86.2	41.7	8.44	0.03	5.60×10^{-7}
	11 1	55.7	138.3	93.8	8.44	0.03	5.60×10^{-7}
	11 2	55.7	74.7	53.0	7.90	0.03	1.41×10^{-7}
	11 3	55.7	49.9	76.1	7.75	0.03	1.75×10^{-7}
	11 4	55.7	127.0	105.3	7.90	0.03	1.41×10^{-7}
	11 5	55.7	103.9	130.1	7.75	0.03	1.75×10^{-7}
	11 6	55.7	40.6	87.9	8.60	0.03	6.08×10^{-7}
	11 7	55.7	92.1	139.4	8.60	0.03	6.08×10^{-7}
	11 8	0.0	113.6	113.6	3.84	0.03	7.40×10^{-6}
	11 14	0.0	66.4	66.4	3.84	0.03	7.40×10^{-6}
	11 9	0.0	165.9	165.9	8.64	0.03	-2.28×10^{-6}
	11 10	0.0	27.8	27.8	7.74	0.03	-2.34×10^{-6}
	11 12	0.0	152.2	152.2	7.74	0.03	-2.34×10^{-6}
	11 13	0.0	14.1	14.1	8.64	0.03	-2.28×10^{-6}

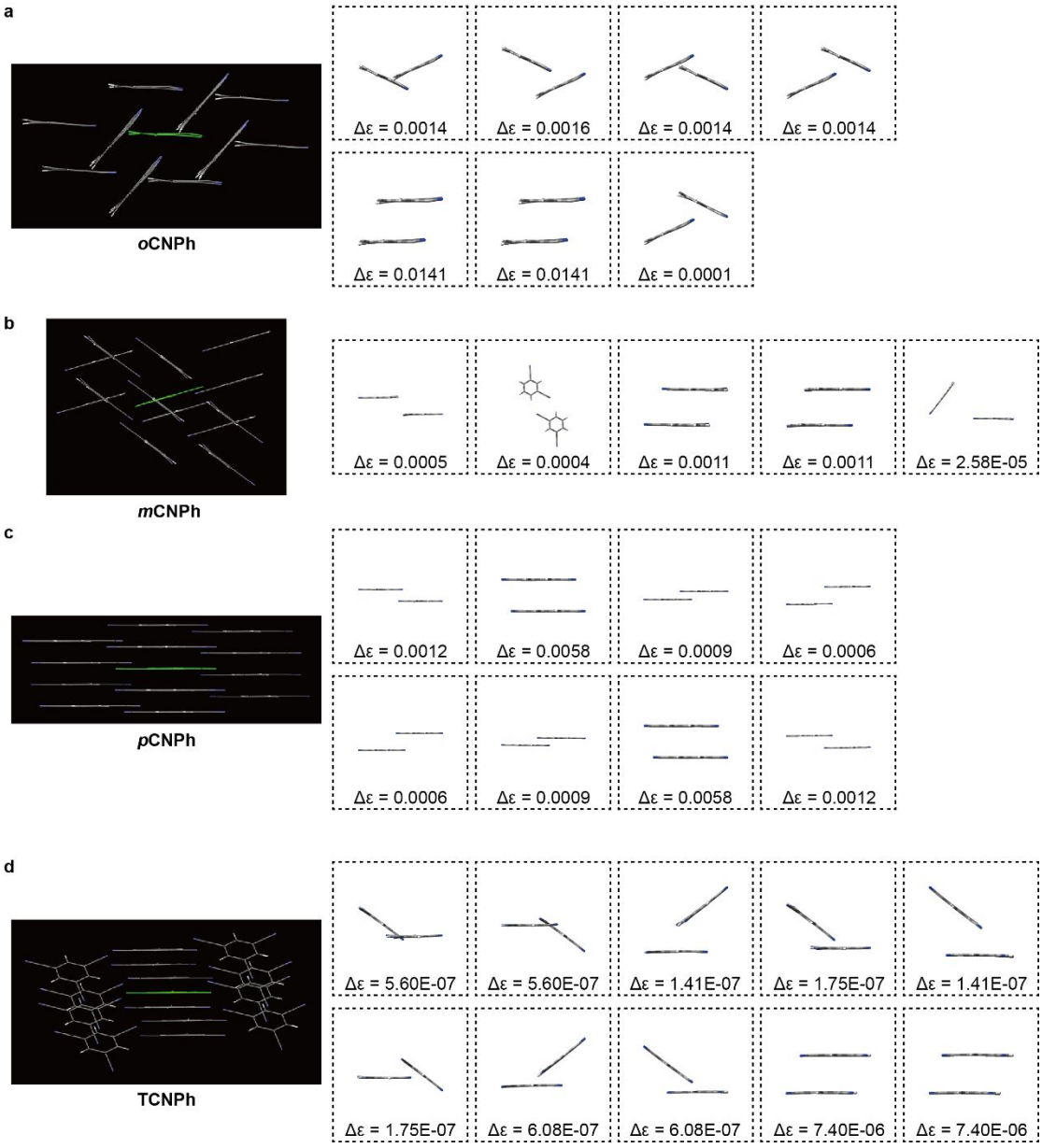

Figure S18. H-aggregates in (a) ***o*CNPh**, (b) ***m*CNPh,** (c) ***p*CNPh** and (d) **TCNPh** single crystals.

Reference

(1) Joo, C. Y.; Soo, Y. K.; Yeob, L. J. A Universal Host Material for High External Quantum Efficiency Close to 25% and Long Lifetime in Green Fluorescent and Phosphorescent OLEDs. *Adv. Mater.* **2014,** *26*, 4050-4055.

(2) Sun, Z.; Luo, J.; Zhang, S.; Ji, C.; Zhou, L.; Li, S.; Deng, F.; Hong, M. Solid-State Reversible Quadratic Nonlinear Optical Molecular Switch with An Exceptionally Large Contrast. *Adv. Mater.* **2013,** *25*, 4159-4163.

(3) Bacon, G. E.; Curry, N. A.; Wilson, S. A.; Spence, R. A Crystallographic Study Of Solid Benzene By Neutron Diffraction. *Proc. R. Soc. A-Math. Phy.* **1964,** *279*, 98-110.

(4) Jung, S.-M.; Kim, D.; Shin, D.; Mahmood, J.; Park, N.; Lah, M. S.; Jeong, H. Y.; Baek, J.-B. Unusually Stable Triazine-based Organic Superstructures. *Angew. Chem. Int. Edit.* **2016,** *55*, 7413-7417.

(5) An, Z.; Zheng, C.; Tao, Y.; Chen, R.; Shi, H.; Chen, T.; Wang, Z.; Li, H.; Deng, R.; Liu, X.; et al. Stabilizing Triplet Excited States for Ultralong Organic Phosphorescence. *Nature Mater.* **2015,** *14*, 685-690.

(6) Lower, S.; El-Sayed, M. The Triplet State and Molecular Electronic Processes in Organic Molecules. *Chem. Rev.* **1966,** *66*, 199-241.

(7) Scott, D. R.; Maltenieks, O. Experimental Method for Determining The Intersystem Crossing Rate Constant from Lowest Excited Singlet to Lowest Triplet State. *J. Phy. Chem.* **1968,** *72*, 3354-3356.

(8) Frisch, M. R.; Trucks, G. W.; Schlegel, H. B.; Scuseria, G. E.; Robb, M. A. Gaussian 09 Gaussian. Inc.: Wallingford, CT, 2009.

(9) Peng, Q.; Shi, Q.; Niu, Y.; Yi, Y.; Sun, S.; Li, W.; Shuai, Z. Understanding the efficiency drooping of the deep blue organometallic phosphors: a computational study of radiative and non-radiative decay rates for triplets. *J. Mater. Chem. C* **2016,** *4*, 6829-6838.

(10) Yang, J.; Zhen, X.; Wang, B.; Gao, X.; Ren, Z.; Wang, J.; Xie, Y.; Li, J.; Peng, Q.; Pu, K.; et al. The Influence of The Molecular Packing on The Room Temperature Phosphorescence of Purely Organic Luminogens. *Nat. Commun.* **2018,** *9*, 840-849.

(11) Birks, J. Excimers. *Reports on progress in physics* **1975,** *38* (8), 903-974.

(12) Schweizer, W. B.; Dunitz, J. D. Quantum Mechanical Calculations for Benzene Dimer Energies: Present Problems and Future Challenges. *Journal of Chemical Theory and Computation* **2006,** *2* (2), 288-291.